B. CHATTERJEE, P. SAHOO

RESEARCH

Elastic-plastic Contact of a Deformable Sphere Against a Rigid Flat for Varying Material Properties Under Full Stick Contact Condition

The present study considers finite element based contact analysis of an elastic-plastic axisymmetric hemisphere using ANSYS to study the effect of material properties under full stick contact condition. Results are compared with previous elastic-plastic models for perfect slip and full stick contact conditions. It is found that materials with modulus of elasticity to yield strength (E/Y) ratio less than and greater than 300 show strikingly different contact behavior. When E/Y ratio is less than 300, contact load increases with the increase in modulus of elasticity whereas in elastic-plastic range, contact load decreases with the increase in yield strength.

Keywords: *Elastic-plastic contact, Full stick, Material properties, Sphere on flat, Finite element method.*

1. INTRODUCTION

Contact is inevitable in engineering applications for transmitting force, motion, power etc through point or line contacts. In the present study, our field of interest is point contact. The study of contact mechanics started with the pioneering work of Hertz [1] who presented the contact analysis of two frictionless (perfect slip) elastic solids with geometries defined by quadratic surfaces. Since then the assumption of surfaces having asperities of spherical shape is adopted to simplify the contact problems. However further progress of Hertz theory did not continue until Huber calculated the stress field developed due to the frictionless spherical contact [2]. Greenwood and Williamson [3] used the Hertz theory and proposed an asperity based elastic model where asperity heights follow a Gaussian distribution. Hertz assumed frictionless surfaces and his theory is restricted to perfectly elastic solids. The first plastic model was introduced by Abbot and Firestone [4]. They neglected the volume conservation of the plastically deformed sphere. The first model of elastic-plastic frictionless contact was proposed by Chang et al. (CEB model) [5]. In this model the sphere remains in elastic contact until a critical interference is reached, above which the volume conservation of the sphere tip is imposed. The CEB model suffers from a discontinuity in the contact load as well as in the first derivative of both the contact load and the contact area at the transition from elastic to elastic-plastic region. Later on, Evseev [6], Chang [7] and Zhao et al. [8] have attempted to improve the elastic-plastic contact model. An introduction of friction at the interface of contact had enabled the Hertz theory to be extended in a realistic manner. Timoshenko and Goodier [9] stated that the results of normal loading under friction differ from the frictionless Hertzian contact problem. However, contact of spheres with same elastic constants yields identical tangential displacements, which eliminates the possibility of interfacial slip and the Hertz theory is applicable in certain cases of frictional contact also [10]. Hence normal contact of two spheres with same material properties exhibits same results under full stick contact and perfect slip contact conditions. This idea is used in modeling spherical contact under combined normal and tangential loading by several researchers [11-14]. These studies [11-14] assumed perfect slip contact during normal loading and used friction for tangential loading. Goodman [15] first provided the analytical solution of two dissimilar elastic spheres in normal contact under full stick (infinite friction) condition. He expressed the distribution of tangential stress over the contact area and ignored

Biplab Chatterjee, Prasanta Sahoo[1]
Department of Mechanical Engineering
Jadavpur University, Kolkata 700032, India
[1]*e-mail: psjume@gmail.com*

the effect of these tangential stresses on the normal displacement. So the pressure distribution over the contact area followed the Hertz result. Spence [16] solved simultaneously the dual integral equations for shear stresses and pressure distribution over the contact area and calculated the total compressive load under full stick condition. Spence [17] extended his previous work for adhesive contact using certain value of friction coefficient. He found that, for the same elastic constants and friction coefficient the extent of slip region is same for specific surface profile. The studies of point contact revealed the effect of contact conditions and material properties on the deformation and stress field. However accurate solutions could not be done until the finite element method was used to solve the problems.

Use of commercial finite element software in contact mechanics came into the existence in the 21st century and it has the capability to calculate accurately the contact parameters like contact load, contact area, and pressure etc. removing some of the assumptions made in the earlier theories regarding asperity interaction and large deformation [18]. Accurate calculations of contact area and contact load are of immense importance in the field of tribology and leads to an improved understanding of friction, wear, thermal and electrical conductance between surfaces. Kogut and Etsion [19] (KE Model) first provided an accurate result of elastic-plastic contact of a hemisphere and a rigid flat using commercial finite element software ANSYS under frictionless contact condition. Jackson and Green [20] (JG Model) extended the KE model to account for the geometry and used five different yield strengths (Y) for their study. Quicksall et al. [21] used finite element technique to model the elastic-plastic deformation of a hemisphere in frictionless contact with a rigid flat for various materials such as aluminum, bronze, copper, titanium and malleable cast iron. They studied the error of formulation for KE and JG models. Shankar and Mayuram [22, 23] used finite element method to study the effect of material properties during transition from elastic to elastic-plastic region with KE model. Recently Malayalamurthi and Marappan [24], Sahoo et al. [25, 26] concluded that the interfacial parameters like contact load, real contact area, during loading are dependent on the material properties of the deformable sphere in contact with a rigid flat. Etsion et al. [27] further extended their study of frictionless contact of a deformable sphere with a rigid flat for analysis of unloading and predicted that unloading is independent of the physical and geometrical properties of the sphere. Jackson et al. [28] studied the residual stress and deformation in elastic-plastic hemispherical frictionless contact with a rigid flat. Malayalamurthi and Marappan [29], Sahoo and Chatterjee [30] also considered the effect of material properties during unloading. So it can be seen that a wide range of literature is available for frictionless contact of a deformable sphere and a rigid flat. The ideal assumption of frictionless contact (perfect slip) may give an idea for interfacial interactions, but results differ from the realistic contact. For example, Johnson [31] observed, "Friction can increase the total load required to produce a contact of given size by at most 5% compared with Hertz."

Two types of contact simulations are in general available in literature; perfect slip and full stick. In perfect slip, it is assumed that there is no tangential stress in the contact area. The contacting points of the sphere and the flat, which are covered by the expanding contact zone, are prevented from further relative displacement in full stick condition [32]. Brizmer et al. [33] first analyzed the effect of full stick condition on the elasticity terminus of a spherical contact using finite element software ANSYS. Brizmer et al. [34] extended their study for the loading of an elastic plastic spherical contact both under full stick and perfect slip contact conditions. They found that interfacial parameters are insensitive to the contact condition and material properties of the deformable sphere. However they concluded that the contact load, average contact pressure is slightly affected by Poisson's ratio. Zait et al. [35] performed the unloading of an elastic-plastic spherical contact under full stick contact condition. They found a substantial variation in load area curve during unloading under full stick contact condition compared to that of perfect slip condition.

An extensive literature review shows that a lot of research has been done to study the effect of material properties on interfacial parameters for perfect slip contact condition and Brizmer et al [33, 34] has provided the accurate solution of contact parameters like contact load, contact area, contact pressure under full stick contact condition using finite element software. However the effect of material properties on contact parameters under full stick contact condition is still not available in the literature. The present study therefore aims to investigate the effect of modulus of elasticity (E), yield strength (Y) and E/Y ratio on contact parameters like contact load, contact area, and contact pressure under full stick contact conditions using the commercial finite element software ANSYS.

2. THEORETICAL BACKGROUND

The contact of a deformable hemisphere and a rigid flat is shown in Fig. 1 where the dashed and solid lines represent the situation before and after contact respectively of the sphere of radius R. The figure also shows the interference (ω) and contact radius (a) corresponding to a contact load (P). As mentioned earlier the present study is concentrated on the full stick contact condition and the results are compared with perfect slip contact condition [26]. Tabor [36] mentioned that full stick contact condition is more realistic than that of perfect slip contact condition due to the formation of junction in the former case. Brizmer et al [34] provided the empirical relations for critical interference and corresponding values for critical loads and critical contact area for perfect slip and full stick contact conditions. For full stick contact condition, the contact parameters (interference ω, load P and area A) are normalized using the following expressions for critical interference (ω_c), critical load (P_c) and critical contact area (A_c) given by of Brizmer et al [34].

$$\omega_c = (C_\nu \frac{\pi(1-\nu^2)}{2}(\frac{Y}{E}))^2 R(6.82\nu - 7.83(\nu^2 + 0.0586)) \quad (1)$$

$$P_c = \frac{\pi^3 Y}{6} C_\nu{}^3 (R(1-\nu^2)(\frac{Y}{E}))^2 (8.88\nu - 10.13(\nu^2 + 0.089)) \quad (2)$$

$$A_c = \pi \omega_c R \quad (3)$$

where, $C_\nu = 1.234 + 1.256\nu$. The parameters Y, E, and ν are the yield stress, Young modulus, and Poisson's ratio of the sphere material, respectively and R is the radius of the sphere.

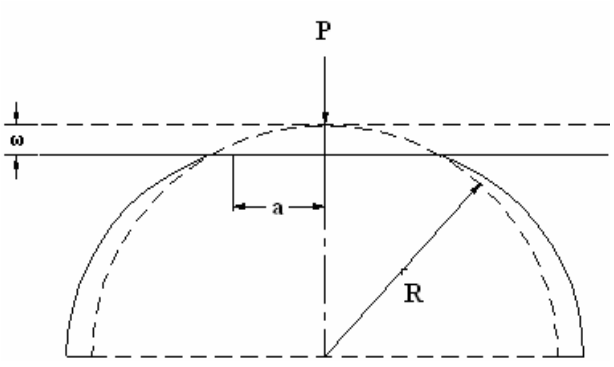

Figure 1. A deformable sphere against a rigid flat

3. FINITE ELEMENT MODEL

The present study utilizes the commercial finite element software ANSYS. To improve upon the efficiency of computation, an axisymmetric 2-D model is used. The hemisphere is modeled by a quarter of a circle, due to its axi-symmetry. A line models the rigid flat. The model refines the element mesh near the region of contact to allow the hemisphere's curvature to be captured and accurately simulated during deformation. The model uses quadrilateral, eight node elements to mesh the hemisphere. The resulting ANSYS mesh is presented in Fig.2. The mesh consists of 12986 no of PLANE82 and 112 no of CONTA172 elements. The rigid flat is modeled by a single, non-flexible two-node target surface element (TARGE169). For full stick contact condition, infinite friction condition is adopted. The mesh is further refined depending upon the requirement for the large deformation.

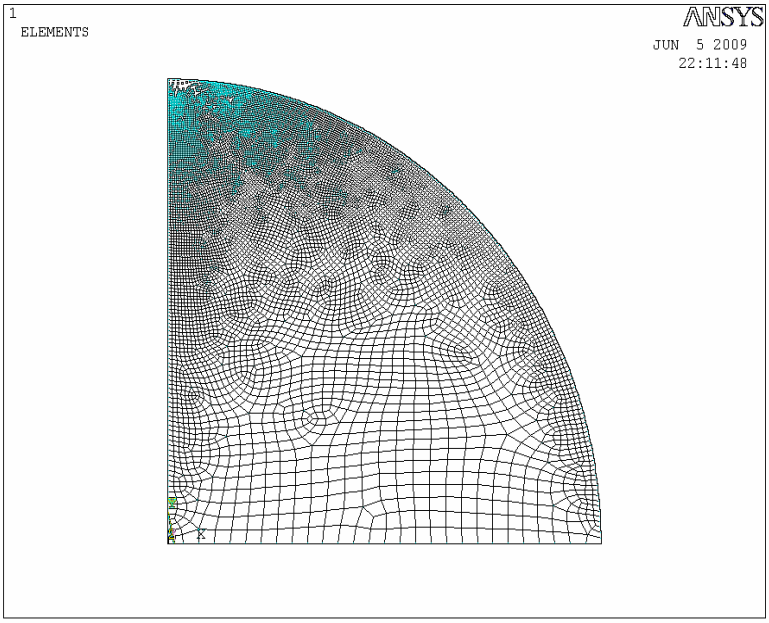

Figure 2. Finite element mesh of the sphere generated by ANSYS

The present work uses a maximum of 16673 elements for the radius of 1 μm. The nodes on the axis of symmetry are fixed in radial direction. Likewise the nodes on the bottom of the hemisphere are fixed in both axial and radial direction. The bilinear isotropic hardening (BISO) option in the ANSYS program is chosen to account the elastic-plastic material response for the single asperity model. The rate independent plasticity algorithm incorporates the von Mises criterion. Tangent modulus is assumed as zero for elastic perfectly plastic models. The mesh density is iteratively increased until the contact force and contact area differed by less than 1% between the iterations. In addition to mesh convergence, the model also compares well with the Hertz elastic solution at interferences below the critical interference for perfect slip contact condition. This work uses Lagrangian multiplier method. The tolerance of current work is set to 1% of the element width. Computations took about 15 minutes for getting solutions up to yield inception and an hour for large deformation in a 1.6 GHz. PC.

4. RESULTS AND DISCUSSION

The deformable sphere with a rigid flat is a fundamental problem to get an insight into the happenings when two rough surfaces will come into the contact. KE [19] provided the general solution for the contact of a deformable sphere with a rigid flat at perfect slip contact condition. Later other authors studied the effect of material properties on contact parameters at perfect slip contact condition. Brizmer et al [34] studied the contact behavior of a deformable sphere with a rigid flat under full stick contact condition. They inferred that the interfacial parameters are slightly affected by Poisson's ratio. They used three values (500, 1000 and 2000) of E/Y (modulus of elasticity to yield strength) ratio. Now Y/E indicates the elastic strain capacity or material strength, thus as E/Y increases, the elastic strain capacity or material strength will decrease. In engineering applications, some alloy steel, high carbon steel, stainless steel are used whose E/Y ratios are below than 300. On the other hand low carbon steel, aluminum, grey cast iron are also widely used with E/Y ratios greater than 300. The present study therefore aims to study the effect of modulus of elasticity, yield strength and E/Y ratio on contact parameters of a deformable sphere with a rigid flat under full stick contact condition. For this purpose, four different values of elastic modulus (E) typical of different steel, aluminum and cast iron are chosen. These are 70, 80, 103 and 200 GPa. Yield strengths are taken as 1.619 and 0.21 GPa. For a yield strength value of 1.619 GPa, the E/Y ratios work out to be 123.53, 63.62, 49.41 and 43.24 respectively. Thus E/Y ratios are less than 300 while for yield strength value of 0.21 GPa, the E/Y ratios are greater than 300. The values of the material parameters are given in Table 1. Poisson's ratio is taken as 0.32. The results of the finite element model are presented for a variety of interferences.

Table 1. Material Properties for different cases

Case	E (GPa)	Y (GPa)	E/Y ratio
1	200	1.619	123.53
2	103	1.619	63.62
3	80	1.619	49.413
4	70	1.619	43.2366
5	200	0.21	952.38
6	103	0.21	490.476
7	80	0.21	380.95
8	70	0.21	333.33

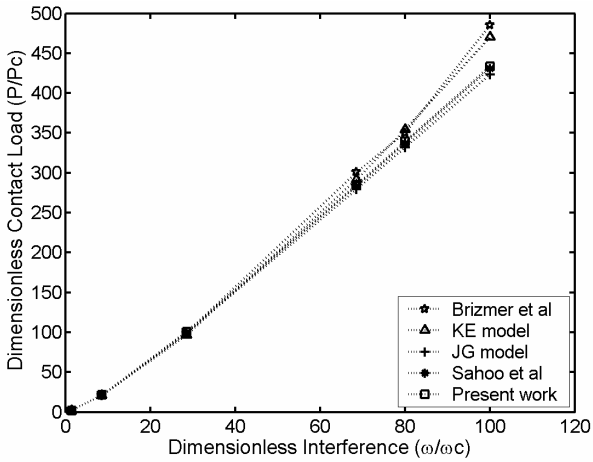

Figure 3. Dimensionless contact load versus dimensionless interference for various models

Fig. 3 presents the comparison of dimensionless contact load (P/Pc) as a function of dimensionless interference (ω/ωc) for various models. KE model [19] presents the contact load in perfect slip contact condition whereas Brizmer et al [34] analyze dimensionless contact load in full stick contact condition. The results from the present simulation under perfect slip contact condition correlate well with the previous studies [20, 26]. In the present study, the emphasis is on contact of an elastic perfectly plastic deformable sphere with a rigid flat under full stick contact condition. Zait et al. [35] also found identical dimensionless contact load for perfect slip and full stick contact conditions during

loading. Present simulation results differ from that of KE model [19] and Brizmer et al [34] because both these studies ignored the effect of low E/Y ratio on contact parameters and used elastic-isotropic linear hardening with a tangent modulus of 2%.

The average contact pressure to yield strength ratio (P/(AY)) as a function of dimensionless interference (ω/ω_c) under full stick contact condition for E/Y<300 is plotted in Fig.4. It is clearly evident from the figure that there is a decrease in mean contact pressure after reaching its peak value, while the peak value is dependent on modulus of elasticity, E. As the value of E increases, peak mean contact pressure also increases. Similar behavior has been observed for perfect slip contact condition also [26].

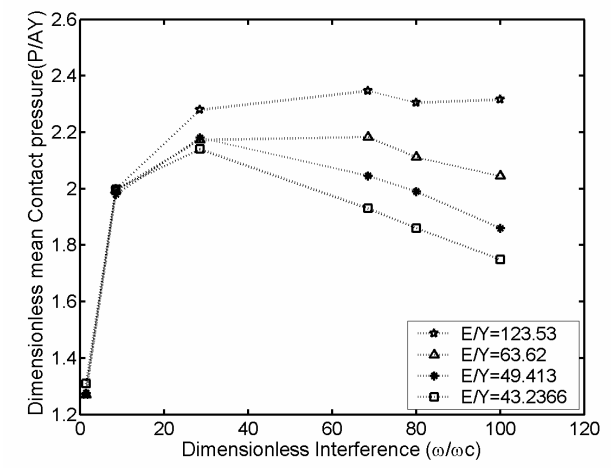

Figure 4. Dimensionless mean contact pressure versus dimensionless interference for E/Y< 300

Fig. 5 represents the plot of dimensionless load (P/P_c) versus dimensionless interference (ω/ω_c) for full stick contact condition when E/Y<300. The dimensionless contact load increases with the increase of E at higher dimensionless interference. At ω/ω_c =100.02, the dimensionless contact load is 36.73%, 20.725%and 7.4% higher for E/Y=123.53, 63.62 and 49.413 respectively than the corresponding value at E/Y=43.2366.

Fig 6 represents the plot of dimensionless contact area (A/A_c) with dimensionless interference (ω/ω_c) when E/Y<300.It is clear from the figure that dimensionless contact area decreases slightly with the decrease in modulus of elasticity. JG model [20] inferred that beyond ω/ω_c= 22, the last contact point displaces positively and those displacement increases with material strength for perfect slip contact condition. For the present stick contact condition, the contact point which tends to displace outward is held back due to the stick contact imposed by the rigid surface.

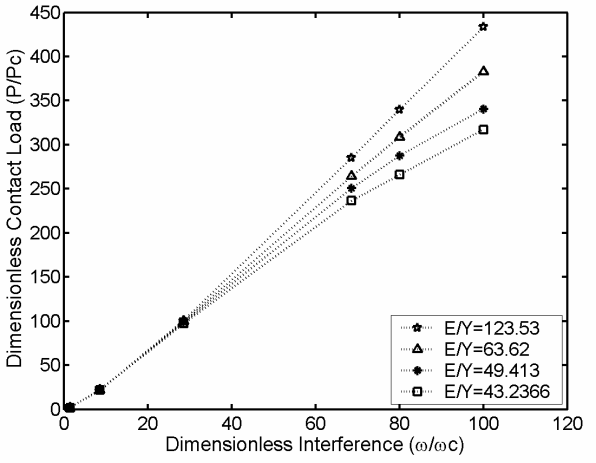

Figure 5. Dimensionless contact load versus dimensionless interference for E/Y<300

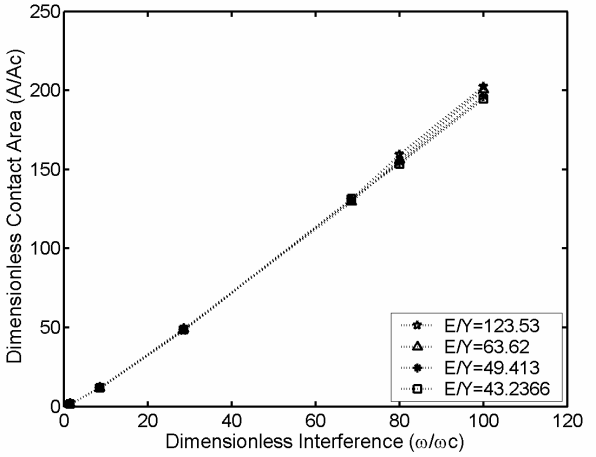

Figure 6. Dimensionless contact area versus dimensionless interference for E/Y<300

Fig. 7 presents the dimensionless contact area (A/A_c) versus dimensionless contact load (P/P_c) for earlier elastic-plastic models under different contact conditions. A comparison is also made with the present simulation. The plots of Brizmer et al under full stick contact and KE model under perfect slip contact condition are obtained from the empirical expressions given in the respective literature. It is found from the plot that the dimensionless contact load is marginally higher under full stick contact condition (Brizmer et al [34]) than that for perfect slip contact (KE model [19]) condition for the same dimensionless contact area. However, the load-area plots for perfect slip [26] and full stick contact (Present work) conditions are nearly identical. This is in conformity with Zait et al. [35] who predicted the same behavior for perfect slip and full stick contact conditions.

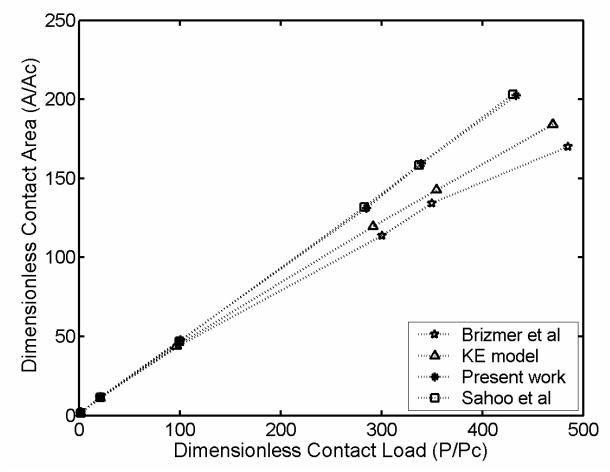

Figure 7. Dimensionless contact load versus dimensionless contact area for various models

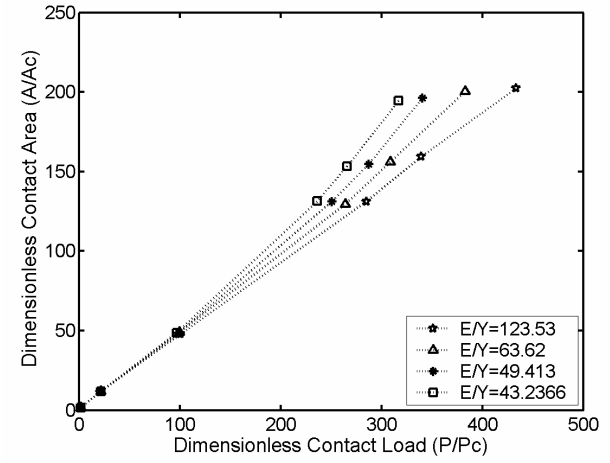

Figure 8. Dimensionless contact load versus dimensionless contact area for E/Y<300

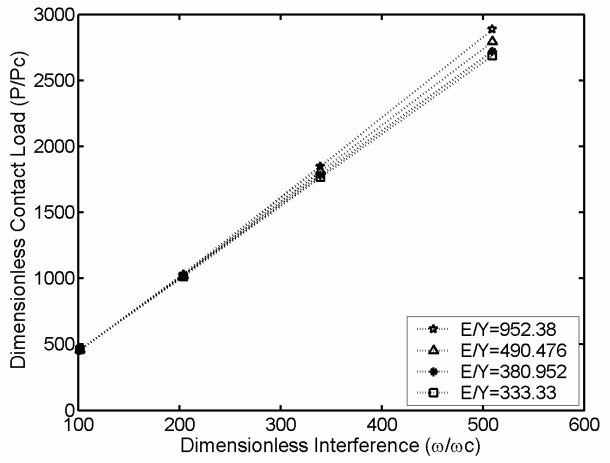

Figure 9. Dimensionless contact load versus dimensionless interference for E/Y>300

Fig 8 presents the dimensionless contact area (A/A_c) versus dimensionless contact load (P/P_c) for full stick contact condition when E/Y ratio is less than 300. It is observed from the figure that with the increase in E/Y ratio the material can support the same applied load in a smaller contact area. Thus the resistance to deformation of a material increases with the increase in E/Y value.

For the second set of simulations, yield strength (Y) is considered at 0.21 GPa. Four different elastic modulus 200, 103, 80, 70 GPa are used and the E/Y ratios are 952.38, 490.476, 380.95, 333.33 respectively (as shown in Table 1). Fig 9 shows the variation of dimensionless contact load (P/P_c) as a function of dimensionless interference ($\omega/\omega c$) when E/Y is greater than 300 under full stick contact condition. It is seen that with the increase of modulus of elasticity (E) the dimensionless load increases in the plastic zone (as evident from the range of ω/ω_c values) and the maximum variation of dimensionless contact load is around 7%.

Fig. 10 shows the results of the dimensionless contact area (A/A_c) as a function of dimensionless interference (ω/ω_c) for full stick contact condition when E/Y> 300. It is clear from the figure that the dimensionless contact area increases slightly with the increase of modulus of elasticity. Fig 11 shows the dimensionless contact area (A/A_c) versus dimensionless contact load (P/P_c) for full stick contact condition when E/Y > 300. It is seen from the figure that when E/Y>300, the contact load-area behavior for stick contact condition does not vary much with modulus of elasticity.

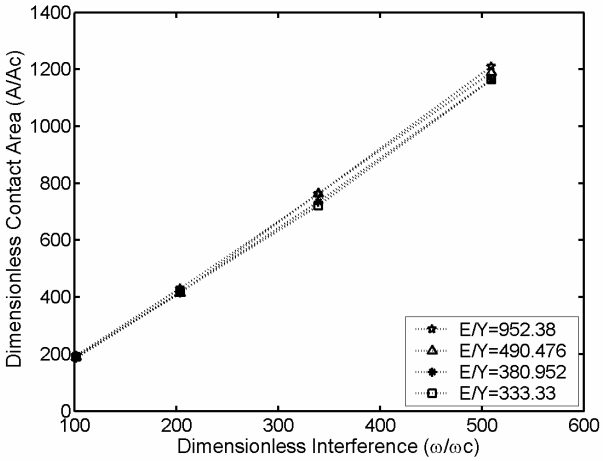

Figure 10. Dimensionless contact area versus dimensionless interference for E/Y>300

It is observed from the previous discussions that contact parameters are strongly affected by material properties when E/Y ratio is less than 300. Now to study the effect of modulus of elasticity and yield strength individually for E/Y<300, four materials with different modulus of elasticity and yield strength are chosen to yield the same E/Y ratio. For this purpose, Ruthenium, Steel, Titanium alloy (ASTM grade-5) and Gold with different modulus

of elasticity and yield strength are chosen and all these have the same E/Y ratio of 120. The properties of these materials are given in Table 2. Fig.12 shows the dimensionless contact area (A/Ac) versus dimensionless contact load (P/P_c) for full stick contact condition for these materials. It may be noted that the load-area behavior is identical for different materials having same E/Y ratio, even though their modulus of elasticity and yield strengths are different. Du et al [37] considered the effect of material properties on adhesive contact of Ruthenium and Gold. They observed that both the materials produced identical dimensionless contact load during loading but only differs during unloading. Thus the present simulation results are in conformity with Du et al. [37].

Table 2. Material properties for four different cases

Material	E (GPa)	Y (GPa)	E/Y
Ruthenium*	410	3.42	120
Steel+	200	1.667	120
Titanium alloy+	105	0.875	120
Gold*	80	0.67	120

* From reference [37], +matweb.com

The present study considers the full stick contact condition for varying modulus of elasticity to yield strength ratios. However, there are other material parameters like Poisson's ratio, work hardening etc. that need to be considered. Also other contact conditions like pure slip and stick-slip need to be considered in future studies. The present study assumes non-adhesive contact situation but a realistic contact analysis should include the presence of adhesion [38]. Future work will consider such contact situations.

5. CONCLUSION

The present work considers 2D axisymmetric finite element model of an elastic perfectly plastic hemisphere in contact with a rigid flat surface for full stick contact condition. The sphere material is modeled as elastic perfectly plastic, and yielding occurs according to the von Mises criterion. The effects of modulus of elasticity, yield strength, and their ratio on interfacial contact parameters are considered in this elastic-plastic model. Comparisons are made with other existing models for perfect slip contact and full stick contact conditions. It is found that dimensionless contact load increases with the increase in modulus of elasticity whereas in elastic-plastic range, the dimensionless contact load decreases with the increase in yield strength. However this phenomenon is not so prominent for the materials with E/Y ratio greater than 300. The contact parameters are strongly affected by the variation in ratio of elastic modulus to yield strength when the ratio is less than 300. However keeping the ratio same, variation in individual values of modulus of elasticity and yield strength does not affect contact parameters significantly.

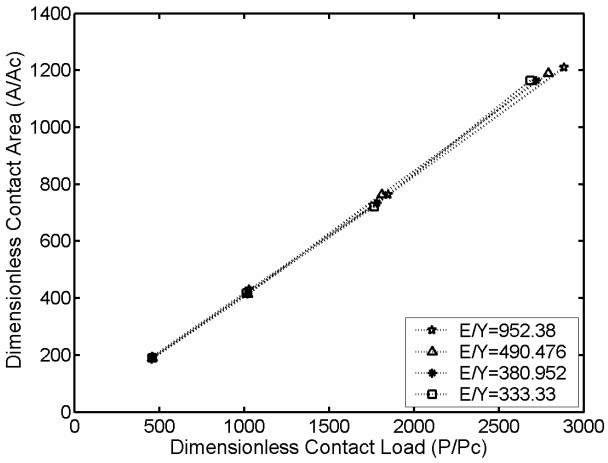

Figure 11. Dimensionless contact load versus dimensionless contact area for E/Y>300

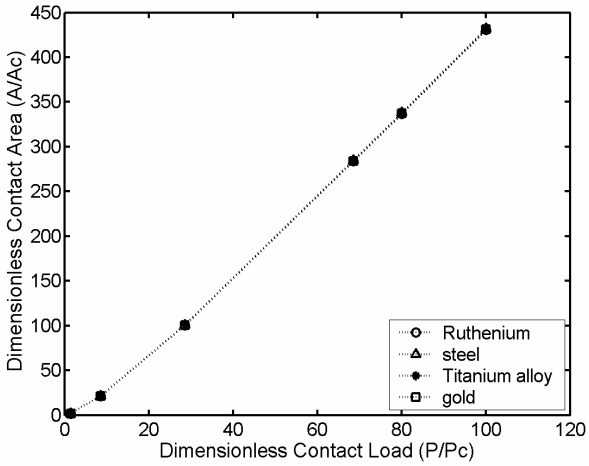

Figure 12. Dimensionless contact load versus dimensionless interference for different materials with E/Y=120

REFERENCES

[1] H. Hertz, *Über die Berührung fester elastischer Köper*, J. Reine and Angewandte Mathematik, Vol. 92, pp. 156-171, 1882.

[2] A.C. Fischer-Cripps, *Introduction to Contact Mechanics*, 2000, Springer, New York.

[3] J.A. Greenwood, J.B.P. Williamson, *Contact of nominally flat surfaces*, Proc. Roy. Soc. London A, Vol. 295, pp. 300-319, 1966.

[4] E.J. Abbott, F.A. Firestone, *Specifying surface quality - a method based on accurate measurement and comparison*, ASME J. Mech. Engg., Vol. 55, pp. 569-572, 1933.

[5] W.R. Chang, I. Etsion, D.B. Bogy, *An elastic-plastic model for the contact of rough surfaces*, ASME J. Tribol., Vol. 109, pp. 257-263, 1987.

[6] D.G. Evseev, B.M. Medvedev, G.G. Grigoriyan, *Modification of the elastic-plastic model for the contact of rough surfaces*, Wear, Vol. 150, pp. 79-88, 1991.

[7] W.R. Chang, *An elastic-plastic contact model for a rough surface with an ion-plated soft metallic coating*, Wear, Vol. 212, pp. 229–237, 1997.

[8] Y. Zhao, D.M. Maietta, L. Chang, *An asperity micro-contact model incorporating the transition from elastic deformation to fully plastic flow*, ASME J. Tribol., Vol. 122, pp. 86–93, 2000.

[9] S.P. Timoshenko, J.N. Goodier, *Theory of Elasticity*, 1970, McGraw-Hill Inc., New York.

[10] K.L. Johnson, *One hundred years of Hertz contact*, Proc. Inst. Mech. Eng., Vol. 196, pp. 363-378, 1982.

[11] R.D. Mindlin, *Compliance of elastic bodies in contact*, J. Appl. Mech. ASME, Vol. 16, pp. 259-268, 1949.

[12] M.D. Bryant, L.M. Keer, *Rough contact between elastically and geometrically identical curved bodies*, J. Appl. Mech. ASME, Vol. 49, pp. 345-352, 1982.

[13] G.M. Hamilton, *Explicit equations for the stresses beneath a sliding spherical contact*, Proc. Inst. Mech. Eng., Vol. 197C, pp. 53-59, 1983.

[14] W.R. Chang, I. Etsion, D.B. Bogy, *Static friction coefficient and model for metallic rough surfaces*, J. Tribol. ASME, Vol. 110, pp. 57-63, 1988.

[15] L.E. Goodman, *Contact stress analysis of normally loaded rough spheres*, ASME J. Appl. Mech., Vol. 29, pp. 515-522, 1962.

[16] D.A. Spence, *Self-similar solutions to adhesive contact problems with incremental loading*, Proc. Roy. Soc. Lond. A, Vol. 305, pp. 55-80, 1968.

[17] D.A. Spence, *The Hertz contact problem with finite friction*, J. Elasticity, Vol. 5, pp. 297-319, 1975.

[18] P. Sahoo, D. Adhikary, K. Saha, *Finite element based elastic-plastic contact of fractal surfaces considering strain hardening*, J. Tribol. and Surf. Eng., Vol. 1, pp. 39-56, 2010.

[19] L. Kogut, I. Etsion, *Elastic-plastic contact analysis of a sphere and a rigid flat*, ASME J. Appl. Mech., Vol. 69, pp. 657-662, 2002.

[20] R.L. Jackson, I. Green, *A finite element study of elastic-plastic hemispherical contact against a rigid flat*, ASME J. Tribol., Vol. 46, pp. 383-390, 2003.

[21] J.J. Quicksall, R.L. Jackson, I. Green, *Elasto-plastic hemispherical contact models for various mechanical properties*, Proc. Instn. Mech. Engrs., Part J: J. Engg. Tribol., Vol. 218, pp. 313-322, 2004.

[22] S. Shankar, M.M. Mayuram, *A finite element based study on the elastic–plastic transition behavior in a hemisphere in contact with a rigid flat*, Journal of Tribology, Vol. 130, pp. 1-6, 2008.

[23] S. Shankar, M.M. Mayuram, *Effect of strain hardening in elastic-plastic transition behavior in a hemisphere in contact with a rigid flat*, International Journal of Solids and Structure, Vol. 45, pp. 3009-3020, 2008.

[24] R. Malayalamurthi, R. Marappan, *Elastic-plastic contact behavior of a sphere loaded against a rigid flat*, Mechanics Advanced Materials and Structure, Vol. 15, pp. 364-370, 2008.

[25] P. Sahoo, B. Chatterjee, D. Adhikary, *Finite element based elastic-plastic contact behavior of a sphere against a rigid flat- effect of strain hardening*, Int. J. Engg. and Tech., Vol. 2, pp. 1-6, 2010.

[26] P. Sahoo, B. Chatterjee, *A finite element study of elastic-plastic hemispherical contact behavior against a rigid flat under varying modulus of elasticity and sphere radius*, Engineering, Vol. 2, pp. 205-211, 2010.

[27] I. Etsion, Y. Kligerman, Y. Kadin, *Unloading of an elastic-plastic loaded spherical contact*, Int. J. Solid Struct., Vol. 42, pp. 3716-3729, 2005.

[28] R. Jackson, I. Chusoipin, I. Green, *A finite element study of the residual stress and deformation in hemispherical contacts*, ASME. J. Tribol, Vol. 127, pp. 484-493, 2005.

[29] R. Malayalamurthi, R. Marappan, *Finite element study on the residual strains in a sphere after unloading from the elastic-plastic*

state, Int. J. Comp. Methods in Engg. Sci. and Mech., Vol. 10, pp. 277-281, 2009.

[30] B. Chatterjee, P. Sahoo, *Effect of strain hardening on unloading of a deformable sphere loaded against a rigid flat- a finite element study*, Int. J. Engg. and Tech., Vol. 2, pp. 225-233, 2010.

[31] K.L. Johnson, *Contact Mechanics*, 1985, Cambridge University Press, Cambridge, MA.

[32] K.L. Johnson, J.J. O' Conner, A.C. Woodward, *The effect of the indenter elasticity on the Hertzian fracture of brittle materials*, Proc. Roy. Soc. Lond. A, Vol. 334, pp. 95-117, 1973.

[33] V. Brizmer, Y. Kligerman, I. Etsion, *The effect of contact conditions and material properties on the elasticity terminus of a spherical contact*, Int. J. Solid Struct., Vol. 43, pp. 5736-5749, 2006.

[34] V. Brizmer, Y. Kligerman, I. Etsion, *The effect of contact conditions and material properties on elastic-plastic spherical contact*, J. Mech. Mater. and Struct., Vol. 1, pp. 865-879, 2006.

[35] Y. Zait, Y. Kligerman, I. Etsion, *Unloading of an elastic-plastic spherical contact under stick contact condition*, Int. J. Solid Struct., Vol. 47, pp. 990-997, 2010.

[36] D. Tabor, *Junction growth in metallic friction: The role of combined stresses and surface contamination*, Proc. R. Soc. London A, Vol. 251, pp. 378-393, 1959.

[37] Y. Du, L. Chen, N.E. McGruer, G.G. Adams, I. Etsion, *A finite element model of loading and unloading of an asperity contact with adhesion and plasticity*, J. Colloid and Interface Science, Vol. 312, pp. 522-528, 2007.

[38] A. Mitra, P. Sahoo, K. Saha, *A multi-asperity model of contact between a smooth sphere and a rough flat surface in presence of adhesion*, Trib. in Industry, Vol 33, No. 1, pp. 3-10, 2011.